Micromagnetic study of magnetic configurations in submicron permalloy disks

Jonathan Kin Ha,* Riccardo Hertel, and J. Kirschner
Max-Planck-Institut für Mikrostrukturphysik, Weinberg 2, 06120 Halle, Germany
(Received 12 July 2002; revised manuscript received 25 November 2002; published 27 June 2003)

We report a finite-element study of magnetic configurations in submicron permalloy disks using micromagnetics principles. Depending on the disk size, many (meta)stable magnetic states such as normal and twisted onion, in-plane vortex, and various buckle states are observed. A diagram is constructed to bring out the dependence of the different remanent states on the disk diameter and thickness. It shows that the disk thickness is the decisive factor in determining whether a vortex state is energetically more favorable than an onion state, and that the disk diameter determines whether some in-plane buckling can be sustainable.

DOI: 10.1103/PhysRevB.67.224432 PACS number(s): 75.75.+a, 75.60.Ch, 75.70.Kw, 75.40.Mg

I. INTRODUCTION

The continuing quest for miniaturation of magnetic elements, which in part is driven by the desire for ever denser data storage media and the promise of faster and more sensitive sensor devices, is made possible by the recent advances in optical[1–3] and electron-beam lithography technologies.[1,4] But as their lateral dimensions shrink to submicron regime, instead of the aggregate of magnetic domains commonly seen in bulk samples or unpatterned thin films, the magnetization can arrange in a *single*, highly nonuniform pattern, examples of which are vortex,[5–10] flower,[11] *S*-, and *C*- states.[10,12] Apart from the interesting spin arrangements, their existence has a significant impact on technological applications, both desirable and undesirable, depending on the particular design of the device. For example, the onset of a vortex state in the active elements of a giant magnetoresistive read head would be detrimental to its operation, even for a simple reason that it would take too large of a magnetic field to switch the magnetization. On the other hand, there have been proposals in the literature about the usage of arrays of submicron ring magnets for ultrahigh density memory storage,[13,14] because such a design naturally promotes a flux closure arrangement (among other advantages), the result of which allows more elements to be closely packed with minimum interference between neighboring rings due to stray field. Hence, as the miniaturation process continues, it is imperative to have a good understanding of the spin arrangement physics, if the current magnetic devices are to continue to operate effectively.

Particularly in the past few years, there has been much discussion on the magnetic states of submicron soft ferromagnetic disks (e.g., Refs. 5,6, and 15, and the references therein), but the attention has been almost exclusively on the ''single-domain'' and vortex states. Our numerical simulations show that other (meta)stable[27] magnetic configurations are possible, including the onion, in-plane vortex, and states of various degrees of in-plane buckling. These states can be accessible by a simple procedure to be described below. A detailed description of each of these magnetic states is an important part of this paper. Insight into peculiar features of a spin arrangement is noted. The effect of disk size on the remanent state is made clear by the construction of a phase diagram. The magnetization processes of these disks have been presented in Ref. 16.

II. SAMPLE SPECIFICATIONS AND NUMERICAL METHOD

The sample material is taken to be permalloy with the magnitude of the saturation magnetic polarization vector $J_s = 1$ T but without any intrinsic anisotropy. The exchange constant A is assumed to be 1.3×10^{-11} J/m. These parameters give the exchange length of 5.7 nm. In this paper, the exchange length is defined as $L_{ex}\equiv\sqrt{A/K_d}$ where $K_d = J_s^2/2\mu_0$. Although real permalloy material usually possesses a weak uniaxial anisotropy, its contribution is excluded in the calculation because we want to keep the physics of nonuniform spin arrangements as simple as possible, while still maintain its essential character. As such, the calculated remanent magnetic configuration is simply the result of the competition between the stray field and exchange energy, the former favoring a closed flux arrangement which necessitates a highly nonuniform spin arrangement due to the sample geometry, the latter favoring uniform magnetization which inevitably generates magnetic poles at the sample surface.

Disks of various diameters and thicknesses are examined. The largest disk diameter in this study is 500 nm, the smallest 50 nm, with different diameter-to-thickness ratio d/t ranging between 1 and 100. The notation used to specify the disk size goes as follows: For example, D200R10 means a disk with a diameter of 200 nm and a diameter-to-thickness ratio d/t of 10.

A finite-element (as opposed to a finite-difference) method is employed to investigate the nonuniformity in the magnetization because of its flexibility in adopting to practically any sample geometry with a high accuracy. The sample is mathematically partitioned into many conformal tetrahedrons, the magnetization in each of which is interpolated linearly based on the values on the four corner points of the tetrahedron. An example of the mesh at the surface of a disk is shown in Fig. 1. The distance between two nodes of a tetrahedron is generally kept between 0.5 to 2 times the material exchange length.[28] Obviously, the decision as to which mesh size to use hinges on the balance between how fine we want to resolve the magnetic structure and how much com-

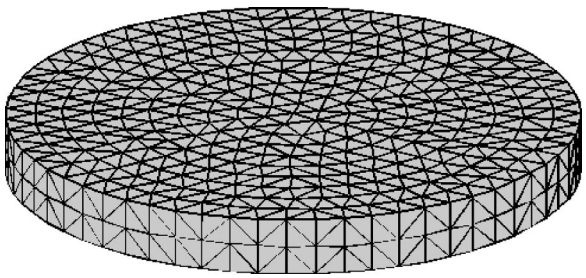

FIG. 1. An example of a finite-element mesh. Only the surface mesh is shown. This particular one is that used to model D100R10.

putation time we are willing to spend. Energy minimum principle is invoked in determining the equilibrium structure. The minimization is achieved by a self-consistent procedure: The stray field is first calculated from an assumed magnetic structure and is subsequently treated as an external magnetic field. The total energy of the system is then minimized via the conjugate gradient path, resulting in a more ''relaxed'' magnetic structure from which the stray field is recalculated. The process repeats until the energy difference between that before and after the minimization is within some specified tolerance. In our computer program code, the stray field is calculated using the hybrid finite element—boundary integral method, first employed by Fredkin and Koehler in solving micromagnetic problems.[17] A more detailed description of our method can be found elsewhere.[18]

III. MAGNETIC CONFIGURATIONS

Different magnetic states are observed, depending on the disk diameter and thickness, and the external field strength and direction. Unless stated otherwise, the magnetic state is prepared by first saturating the magnetization in a large in-plane magnetic field. The field strength then decreases gradually, typically in 1 mT step size. The naming of a magnetic configuration (e.g., onion, vortex, etc.) is based on the *in-plane* arrangement of the magnetization, simply because the pattern is strongly influenced by the circular in-plane geometry, particularly for disks whose aspect ratio $d/t \ll 1$. Also, to facilitate the discussion below, a Cartesian coordinate system is introduced with the *z* axis pointing in the disk normal direction, and the *x*-axis along the external field. The origin of the coordinates is positioned at the center of the disk. Lastly, the notations m_x, m_y, and m_z are used to denote the vectorial components of the normalized magnetization vector along the *x*, *y*, and *z* axes, respectively.

A. Normal onion states

Figure 2 shows an example of what we call a normal onion state (as opposed to a twisted one to be described later). In particular, it is the magnetic state observed in D200R20 at 10-mT field. This magnetic configuration has a clear mirror axis of symmetry about the *x* axis, which is selected out by the external magnetic field. About the symmetry or onion axis, the in-plane magnetization is quite uniform. But in the regions at about $\pm 45°$ away from the direction of the symmetry axis [these are the four blue ''corners'' shown in Fig. 2(a)], some curling is observed. The deviation from the uniform arrangement is driven by the need to minimize the amount of poles created at the perimeter of the disk. The nonuniform characteristics is made more obvious in Fig. 2(b) by plotting the *y*-component of the magnetization, which shows a substantial variation, with m_y ranging between ± 0.47.

Interestingly, there is a sizable out-of-plane component of the magnetization near the ''head'' and ''tail'' of the onion axis, as shown in Fig. 2(c). In this particular pattern, the value of m_z peaks around 0.07, which corresponds to the canting of the magnetization at about 4° with respect to the disk surface. In some thicker disks, a much more pronounced magnetization canting can be seen (for example, to about 13° in D200R10 at 11 mT field). The opening/closing of the magnetization or the flowering effect in the *z* direction can be understood by noting that the system, in so doing, can have a better flux closure outside the sample. Remarkably, these two mechanisms, namely the ''flowering'' and ''onionization'' processes, which are ways to reduce stray field, do not compete with each other, not because the former affects strictly the out-plane-plane components of the magnetization, the latter the in-plane, but because the two processes are most effective in different regions of the magnetic pattern. For this reason, it is often the case that both characteristics are present in an onion state.

The onion state is often referred to as a ''single-domain'' state in the literature. We feel that such a negligence of its onionic character is too crude. This is particularly evident in the study of magnetization process in which even the presence of some degree of onionicity can significantly enhance the switching field of the particle via the so-called configurational anisotropy[11] or configurational stability.[16] As a rule of thumb, a single-domain state is more stable than an onion state only if the disk diameter is less than the exchange length (which is about 5.7 nm for permalloy); otherwise, some degree of nonuniformity would be inevitable in an effort to reduce the stray field energy (Ref. 19, p. 180). Incidentally, the name ''onion'' is used to describe this magnetic state because of its resemblance to a cross-sectional view of an onion that is sliced through the center from top to bottom.[29]

B. Vortex states

In a vortex state, the magnetization essentially aligns with the disk geometry as much as possible in an effort to achieve a zero flux leakage condition. This results in a spiral arrangement of the spins or a vortex, with the magnetization winding either out of or in the disk plane at the vortex core. If the core axis lies in the disk plane, it is an in-plane vortex; if it points perpendicular to the disk plane, it is a out-of-plane vortex, for the obvious reason. Needless to say, the zero-flux state is achieved at the hefty expense of the exchange energy.

Figure 3(a) shows a top view of the out-of-plane vortex state observed in D400R10 in zero field. The core of the vortex is clearly seen to lie perpendicular to the disk plane. A cross-sectional view of the plane, cutting normal to the disk plane and through the vortex core, is depicted in Fig. 3(b).

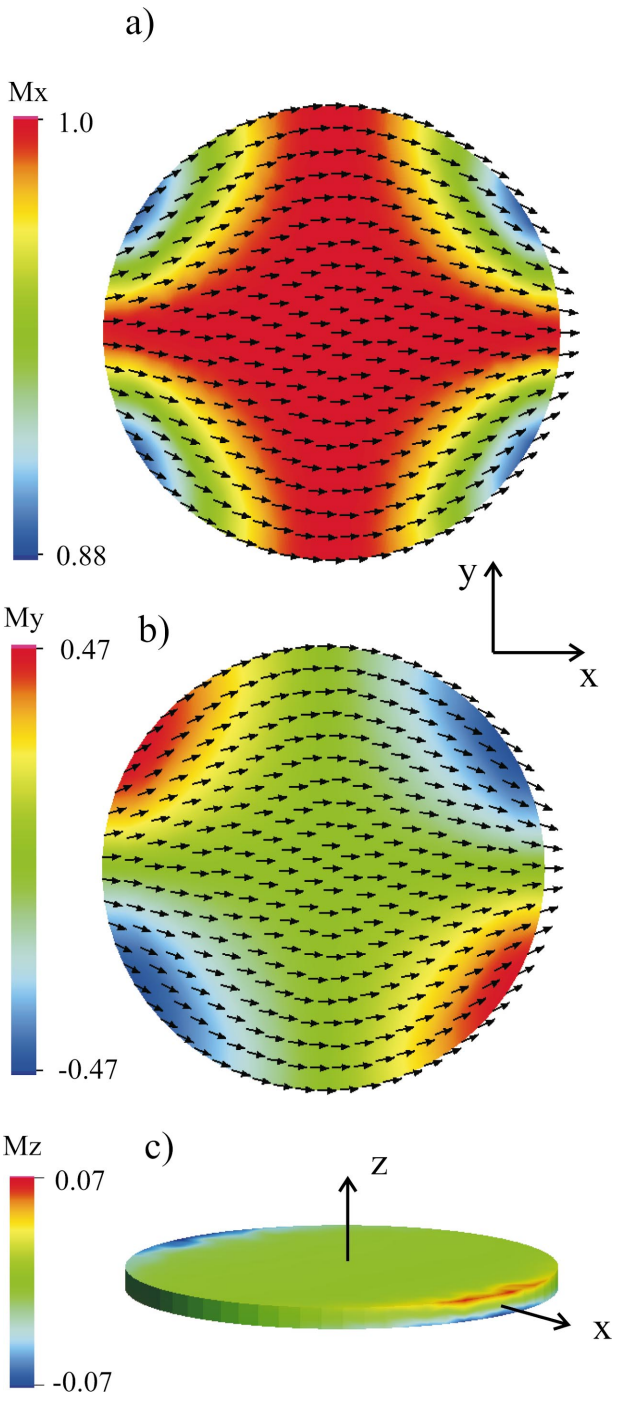

FIG. 2. (Color) Normal onion state observed in D200R20 at 10-mT field. Both (a) and (b) are top views of the disk, with the color coatings reflecting the variation in the x and y components of the magnetization, respectively. The arrows are the projection of the magnetization onto the disk surface. Part (c) is a perspective view of the disk with the color reflecting the variation in the z component of the magnetization.

Note that the size of the core region decreases as it proceeds toward the disk surface, and this is made particularly obvious by the contour lines. The bottle-neck effect is simply a consequence of the need to reduce surface charges. The magnetization profile along the line through center of the disk, as

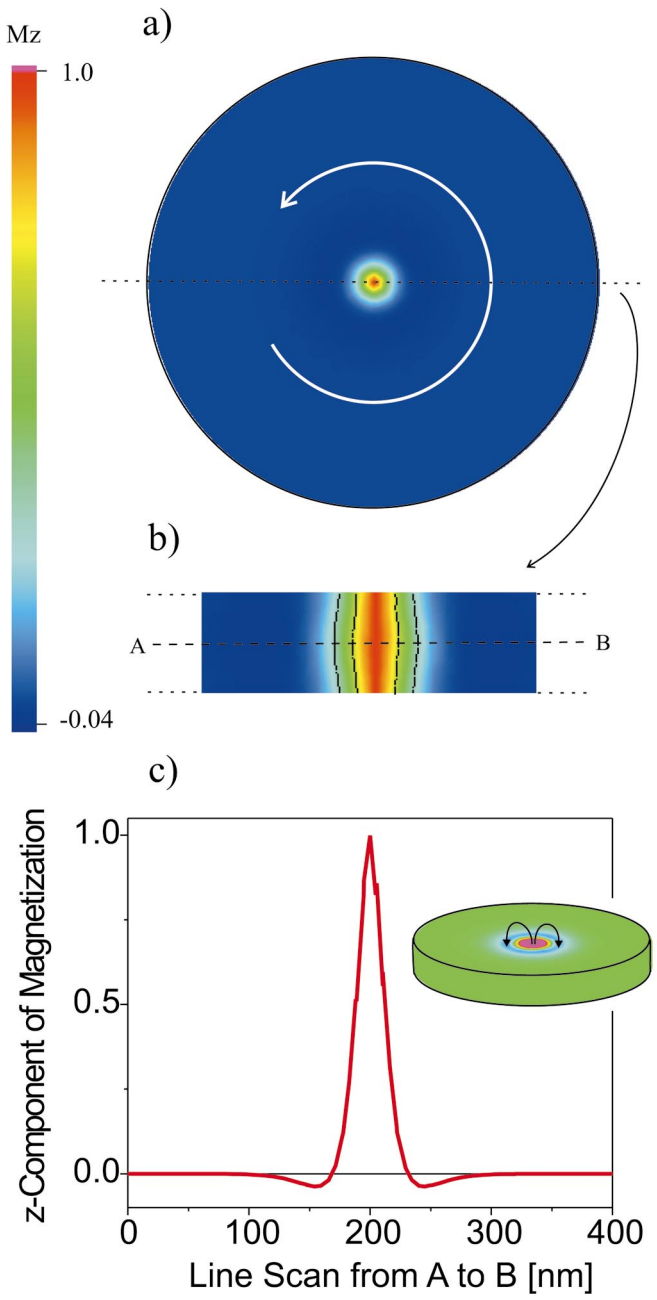

FIG. 3. (Color) Out-of-plane vortex state observed in D400R10 at zero field. The color coating reflects the z component of the magnetization. (a) A top view of the magnetic state. (b) Only a *portion* of the cross-sectional plane cutting normal to the disk surface and through the center of the disk is shown; the dashed lines near the core are the contour lines, that is, lines of constant m_z in this case. (c) The out-of-plane component of the magnetization along the line *AB*, as indicated in (b), is plotted. The inset shows the vortex state in perspective with the same color spectrum used in part (a) to map the variation of m_z between ± 0.04. The two bending arrows are to indicate schematically the field lines between the positive charge at the core and the concentric band of negative charge encircling it.

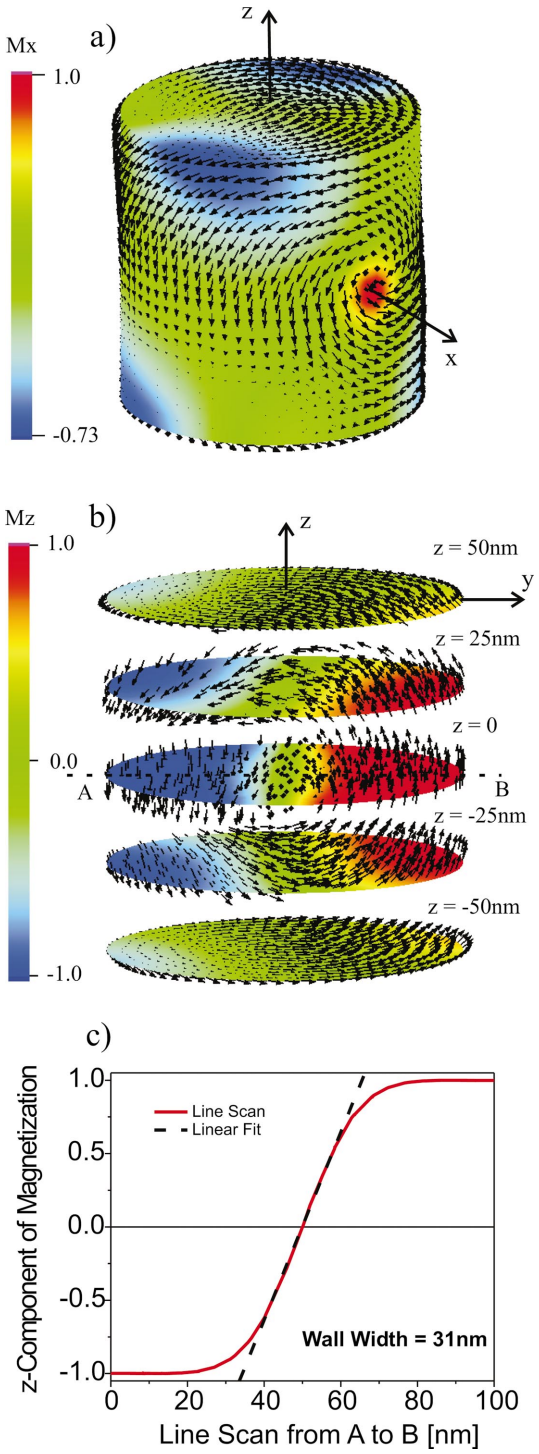

FIG. 4. (Color) In-plane vortex state observed in D100R1 at zero field. (a) A perspective view of the vortex state; the color coating reflects the variation of the *x* component of the magnetization. (b) Five cross-sectional planes of the disk at different *z* positions: 50, 25, 0, -25, and -50 nm. The color coating corresponds to the variation of the *z* component of the magnetization. (c) The *z* component of the magnetization along the line *AB*, as indicated in (b), is plotted. By fitting a linear line using the slope of the wall profile at the disk center, the wall width is estimated to be about 31 nm.

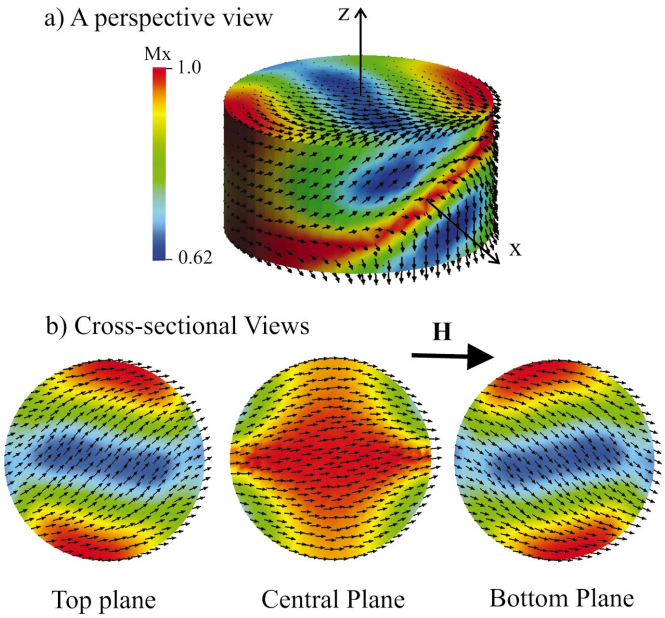

FIG. 5. (Color) Twisted onion state observed in D200R2 at 162-mT field; the color reflects the variation in the *x* component of the magnetization: (a) a perspective view; (b) three cross-sectional views of the planes at z=50, 0, and -50 nm.

indicated by the dashed line *AB* in the cross-sectional plane [part (b) of the figure], is plotted in Fig. 3(c). If the core region is taken to be that in which the magnetization cants less than 45° away from the disk normal axis, its radius is found to be about 15 nm for this particular magnetic structure. Lastly, it is interesting to observe a ''dip'' in the magnetization near the core area in the line scan. This dip is part of a concentric band of negative charge surrounding the positive charge at the core, as it is shown in the inset of Fig. 3(c). The charged band provides a closed flux path to the core magnetic field, and has also been reported by Raabe *et al.*[20] It should be mentioned that this type of vortices, the type with the vortex axis pointing out of the disk plane, has been observed experimentally and theoretically in cobalt and permalloy disks (e.g., Refs. 15 and 21), and recently in Fe islands using a spin-polarized scanning tunneling technique.[22]

Figure 4(a) also shows a perspective view of the in-plane vortex state observed in D100R1 in zero field. Contrary to the out-of-plane vortex state, the core axis lies in the disk plane. Figure 4(b) shows a series of cross-sectional views of planes parallel to the disk surface. Starting from the center of the disk, the magnetic arrangement is that of a Bloch-wall pattern, with two domains pointing out of the disk plane but in opposite direction and a Bloch wall separating them. The width of the Bloch wall can be calculated by monitoring the *z* component of the magnetization along the line *AB* indicated by the dashed line shown in the figure. The result is plotted in Fig. 4(c). Using the Lilley method (Ref. 19, p. 219), which linearizes the wall profile with the slope taken from that at its inflection point, the Bloch wall width is found to be about 31 nm. Incidentally, if it were a true Bloch wall, its width would have been $\delta = \pi\sqrt{A/K_d} = 18$ nm. Toward the disk surface, the magnetization becomes more in plane, but with a sizable out-of-plane component retaining even at the

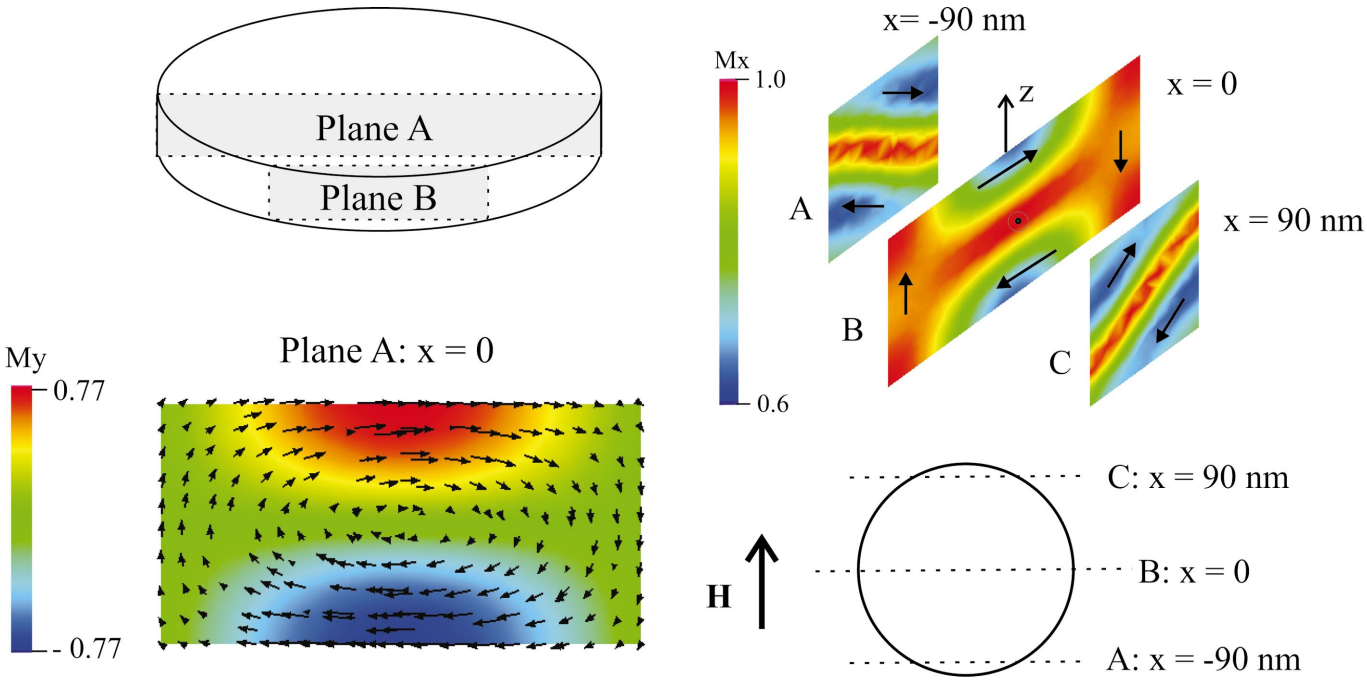

FIG. 6. (Color) Two cross-sectional views of the spin arrangement of D200R2 at 162-mT field. The two planes cut normal to the disk surface, one at $x=0$, the other 90 nm. The color reflects the variation of a component of the magnetization. The arrows are the projection of the magnetization on the yz plane.

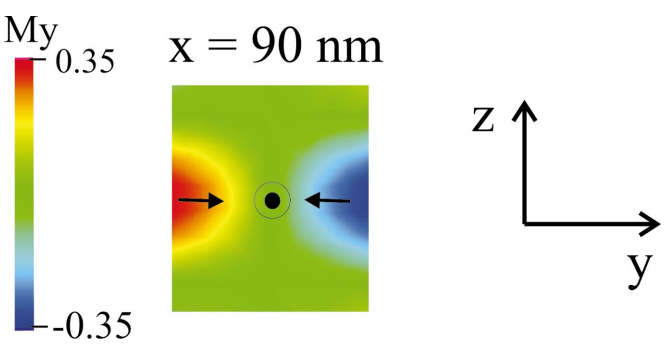

FIG. 7. (Color) A head-on domain pattern observed in in D200R2 at 202-mT field.

FIG. 8. (Color) Three cross-sectional views of the spin arrangement of D200R2 at 162-mT field.

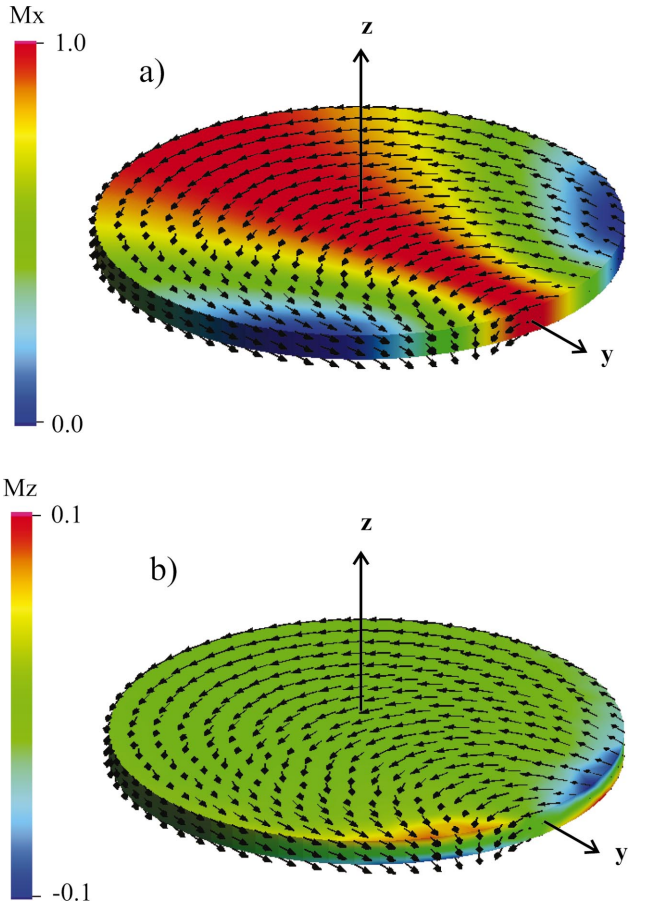

FIG. 9. (Color) Perspective views of a *C* state observed in D200R20 at 0-mT field. The color in (a) shows the variation in the x component of the magnetization, in (b) that in the z-component.

surface of the disk, as much as $\pm 0.6 J_s$ in some parts of the configuration. The in-plane component of the magnetization at the surface also arranges in a nonuniform pattern, similar to that of an onion state, in that the spins curl to adopt the circular disk geometry as much as possible to minimize the stray field energy generated by surface poles.

C. Twisted onion states

Figure 5(a) shows a perspective view of what we call a twisted onion state. It is the magnetic state observed in D200R2 at 162 mT field. This is a complex structure which, like other complicated entities, requires some analytical incisions to make some sense of it. Perhaps the first logical cut is to examine the projected magnetization on the cutplane parallel to the disk surface through the disk center as shown in Fig. 5(b). This magnetic pattern on the central plane is unmistakably that of an onion state. The magnetization on other planes, those parallel to this central plane, stays more or less an onion pattern but with its onion axis progressively ''twisted'' in the opposite direction as it moves toward the top and bottom surfaces of the disk [see Fig. 5(b)]. To see the reason for the twisting of the onion axis, Fig. 6 shows the projected magnetization on two planes cutting normal to the disk surface, one at $x=0$ (plane A), the other at $x=90$ nm (plane B). Some flux closure is clearly seen in both patterns, suggesting the collapse from a normal to a twisted onion state is derived, at least in part, by the saving of the stray field energy. The flux closure results in an elliptical vortex pattern on these planes. Its being elliptical, as opposed to circular, is simply because the aspect ratio d/t is less than one in this particular disk.

It is interesting to note the tendency of the major axis of the ellipsoidal pattern on planes parallel to A, to cant away from the y-axis toward its diagonal. Why is there a need for such a canting? One possible explanation is that the system does it to avoid an otherwise head-on domain configuration in the y component of the magnetization. Figure 7 shows an example of such a pattern observed in the same disk but at a higher magnetic field (e.g., 202 mT), as part of a normal onion structure.[30] The y component near the wall region creates like charges which repel one another, the existence of which is energetically unfavorable. But such a costly arrangement can be avoided if the two domains of the head-on domain pattern are to rotate away oppositely from each other and out-of-plane, as that done in plane B of Fig. 6(b). This may indeed be the leading force that drives the transformation from a normal to a twisted onion state. Along the same line of reasoning, we can expect to see more canting of the ellipsoidal axes in regions that favor larger y component by the disk geometry, and this is in fact what is observed in the simulation.

Equally interesting to observe, as shown in Fig. 8, is that the vortex major axis cants oppositely as it approaches the head and tail of the onion state. This occurs because the sense of the vortex dictates the direction in which the ellipsoidal axes of the vortex should cant. Take the vortex on the central plane (plane B) as the reference. On planes to the head of the onion (e.g., plane C), the rotation of the ellipsoidal axes must be opposite to the sense of the vortex on the central plane, in order for preserve the sense of the vortex. On planes to the tail of the onion (e.g., plane A), the ellipsoidal axes must rotate in the same direction as the sense of the vortex on the central plane. This opposite canting characteristic is the resolution of otherwise head- and tail- on domain patterns on the head- and tail- sides of a normal onion state, respectively. Coincidentally, this doing also provides the best flux closure between poles at the top surface and those at bottom of the disk within the constraint of the configuration.

D. In-plane buckle states

All of the patterns presented so far can be fitted into two broad categories, namely onion and vortex. They are the two extremes of the spectrum of all possible spin arrangements in these submicron disks. On the one side is the onion pattern which is heavily dictated by the exchange interaction that favors uniformity in the spin distribution. The twisted onion state also belongs to this broad category, for its average magnetization remains overwhelmingly in the x direction (e.g., $\langle m_x \rangle = 0.86$ in the configuration discussed earlier in Fig. 5). On the other side is the vortex pattern which is heavily dictated by the need to save the stray field energy, to have as little flux leakage as possible. However, there are intermediate states, ones that are neither highly uniform nor highly spread, as the result of a compromise between the exchange and stray field energies. Buckle states, that is, states in which the in-plane magnetization buckles, are good examples of this class of spin arrangement.

Many degrees of buckling, based on the number of ''oscillations'' in the in-plane magnetization, can be identified. The first-order buckling, as shown in Fig. 9, is what we call a C state, because of its resemblance to the letter C of the Latin alphabet. From the view point of the stray field energy, this pattern has the advantage over the onion in that the magnetic poles of both polarity are situated near the opening ends of the C pattern, resulting in the stray field quite compactly confined to a rather limited area outside the sample. Further examination, as shown in Fig. 9, reveals some degree of flowering also present in the vicinity of these surface poles, for the same reason as that in the onion state, namely to provide a better flux closure outside the sample. It is intriguing, though not surprising, to see in Fig. 9(b) that the opening and closing of the magnetization are coordinated in such a way that gives rise to poles of opposite polarity as close as possible, and those of same polarity as far as possible, within the constraint of the C-state pattern.

An example of second-order buckling is shown in Fig. 10. The pattern is called the S-state, for the obvious reason like that of the C state. A third-order buckle state—we can call it the W state—is shown in Fig. 11. Detailed discussion of these patterns will be presented elsewhere. Incidentally, it should be mentioned that no out-of-plane buckling is observed in any of the disks discussed in this paper simply because it is too thin (less than 100 nm) to support it. Lastly, we would like to acknowledge that bucklings of first and second order (though not so named) have recently been reported by Guslienko *et al.*[21]

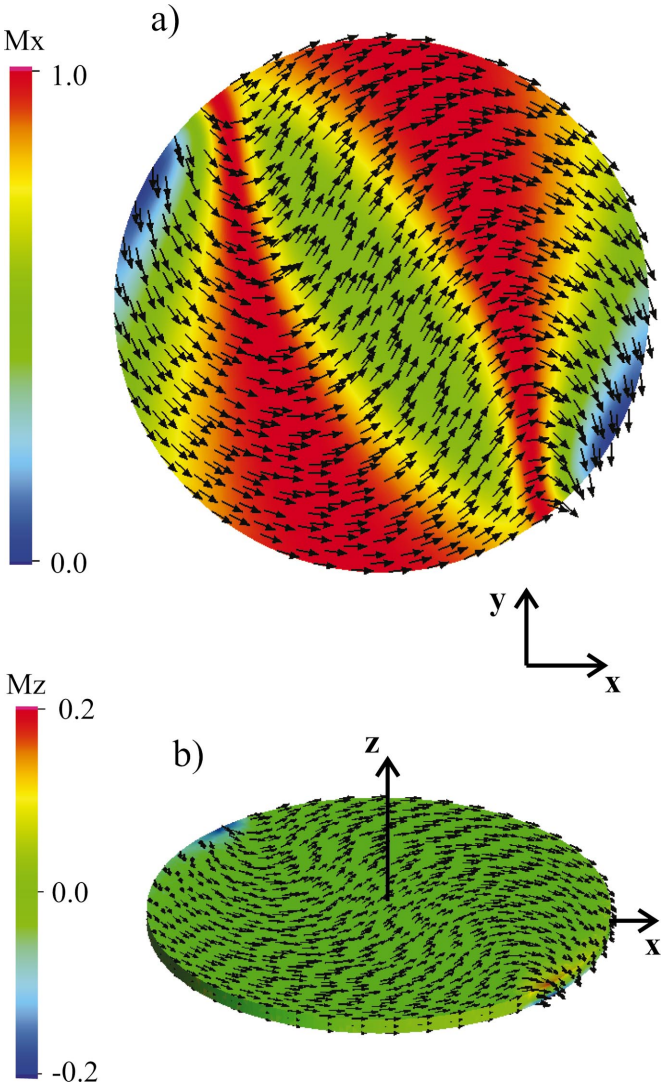

FIG. 10. (Color) Second-order buckle state observed in D500R30 at 3-mT field. (a) A top view of the $x=0$ plane with the color reflecting the variation in the x-component of the magnetization. (b) A perspective view showing the variation in the z component of the magnetization.

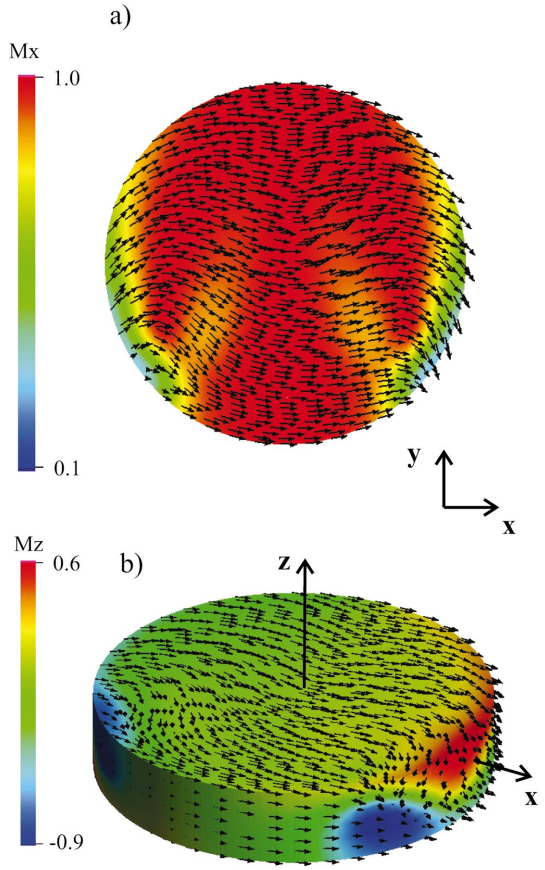

FIG. 11. (Color) Third-order buckle state observed in D400R5 at 89-mT field. (a) A top view. (b) A perspective view.

IV. DIAGRAM OF REMANENT STATES

Thus far, different magnetic configurations observed in these submicron disks have been presented. But it would be instructive to have a diagram that brings out the evolution of the different magnetic states as functions of disk diameter and thickness. Figure 12 is such a diagram, constructed for the remanent states which are obtained by the procedure stated before, that is, start with the magnetization in saturation by a large external field, and then the field gradually decreases to zero strength. However, there is a caveat which should be made clear before we proceed. The red-coated data in the diagram are not really remanent states—not quite. Their true remanent patterns are onions, but these onion states collapse into the indicated states as soon as the field reverses its polarity (less than 1-mT field strength). Because the simulation results assume zero thermal fluctuation and that the sample is always perfectly aligned, both of which

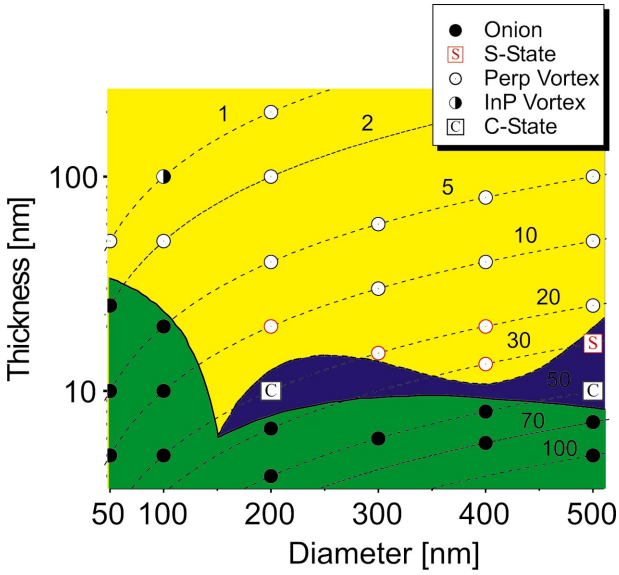

FIG. 12. (Color) A diagram showing the remanent states of different disk diameters and thicknesses. The red-coated data points are not true remanent states, as it is explained in the text. The dashed lines are the iso-ratio lines; that is, lines of constant aspect ratio. The solid lines are the boundaries separating the different magnetic phases. They are drawn with the guide of the eye.

conditions are typically not satisfied in experimental settings, these indicated states might as well be those observed in remanence due to these non-ideal conditions. Besides, the phase diagram would not have been as instructive if they were replaced with that of an onion.

With the caveat aside, three broad regimes are clearly demarcated on the phase diagram: disks whose diameter and thickness fall into the green region have the onion pattern in remanence; those in the yellow have the vortex pattern; and those in the blue area show in-plane buckling. Although the exact boundary between the different regimes cannot be marked precisely due to the limited number of the data points shown on the figure, its trend and general look are clear and would only be refined, not altered, with more data points. Note that disks of aspect ratio less than one (that is, pillars and nanowires) have not been studied in this paper but been explored by Ross *et al.* as reported in Ref. 23.

The remanent-state diagram also shows clearly that the aspect ratio d/t is certainly not the major factor in determining the remanent states of the system. If it were, the states on the same isoratio line—line of constant aspect ratio d/t, the dashed lines shown on the figure—should have a same magnetic pattern (e.g., onion, or vortex, and so forth), which is clearly not so. It is the thickness of the disk that plays a decisive role in determining whether a vortex state is energetically more favorable than an onion state, and the disk diameter that determines whether some buckling is sustainable.

It may strike the reader as being peculiar that only D100R1 is reported to have a stable in-plane vortex state at its remanence. However, this does not mean that the in-plane vortex state can not be stabilized in other disks. Indeed, it can be if an external field is present, as in D200R1 at 125-mT field.

V. SUMMARY

In this paper, we have presented various (meta)stable magnetic patterns in Permalloy disks, including normal and twisted onion states, in-plane vortex state, and states with various degrees of in-plane buckling. The study of the magnetic pattern of these states is interesting in itself. Their identification is crucial in understanding the magnetization processes in these submicron disks. A diagram of remanent states has been constructed to show the dependence of the different remanent states on the disk diameter and thickness.

*Electronic address: kha@mpi-halle.mpg.de

[1] C. Fermon, *Spin-Electronics* (Springer, New York 2001), Chap. 16, p. 379.
[2] C. Ross, Annu. Rev. Mater. **31**, 203 (2001).
[3] O. Fruchart, J.P. Nozières, B. Kevorkian, J.C. Toussaint, D. Givord, F. Rousseaux, D. Decanini, and F. Carcenac, Phys. Rev. B **57**, 2596 (1998).
[4] B. Khamsehpour, C.D.W. Wilkinson, J.N. Chapman, and A.B. Johnston, J. Vac. Sci. Technol. B **14**, 3361 (1996).
[5] R.P. Cowburn, D.K. Koltsov, A.O. Adeyeye, M.E. Welland, and D.M. Tricker, Phys. Rev. Lett. **83**, 1042 (1999).
[6] K.J. Kirk, S. McVitie, J.N. Chapman, and C.D.W. Wilkinson, J. Appl. Phys. **89**, 7174 (2001).
[7] M. Hehn, K. Ounadjela, J.-P. Bucher, F. Rousseaux, D. Decanini, B. Bartenlian, and C. Chappert, Science **272**, 1782 (1996).
[8] R.E. Dunin-Borkowski, M.R. McCartney, B. Kardynal, and D.J. Smith, J. Appl. Phys. **84**, 374 (1998).
[9] T. Shinjo, T. Okuno, R. Hassdorf, K. Shigeto, and T. Ono, Science **289**, 930 (2000).
[10] R. Hertel and H. Kronmüller, Phys. Rev. B **60**, 7366 (1999).
[11] M.E. Schabes and H.N. Bertram, J. Appl. Phys. **64**, 1347 (1988).
[12] Y. Zheng and J.-G. Zhu, J. Appl. Phys. **81**, 5471 (1997).
[13] J.-G. Zhu, Y. Zheng, and G.A. Prinz, J. Appl. Phys. **87**, 6668 (2000).
[14] S. Li, D. Peyrade, M. Natali, A. Lebib, Y. Chen, U. Ebels, L.D. Buda, and K. Ounadjela, Phys. Rev. Lett. **86**, 1102 (2001).
[15] R.P. Cowburn, J. Phys. D: Appl. Phys. **33**, R1 (2000).
[16] J.K. Ha, R. Hertel, and J. Kirschner, Phys. Rev. B **67**, 064418 (2003).
[17] D.R. Fredkin and T.R. Koehler, IEEE Trans. Magn. **26**, 415 (1990).
[18] R. Hertel, J. Appl. Phys. **90**, 5752 (2001).
[19] A. Hubert and R. Schäfer, *Magnetic Doamins—the Analysis of Magnetic Microstructures* (Springer, New York, 1998).
[20] J. Raabe, R. Pulwey, R. Sattler, T. Schweinböck, J. Zweck, and D. Weiss, J. Appl. Phys. **88**, 4437 (2000).
[21] K.Y. Guslienko, V. Novosad, Y. Otani, H. Shima, and K. Fukamichi, Phys. Rev. B **65**, 024414 (2001).
[22] A. Wachowiak, J. Wiebe, M. Bode, O. Pietzsch, M. Morgenstern, and R. Wiesendanger, Science **298**, 577 (2002).
[23] C.A. Ross *et al.* Phys. Rev. B **65**, 144417 (2002).
[24] J. Rothman, M. Klaui, L. Lopez-Diaz, C. Vaz, A. Bleloch, J. Bland, Z. Cui, and R. Speaks, Phys. Rev. Lett. **86**, 1098 (2001).
[25] R. Hertel and H. Kronmüller, J. Appl. Phys. **85**, 6190 (1999).
[26] R.D. McMichael and M.J. Donahue, IEEE Trans. Magn. **33**, 4167 (1997).
[27] About the issue of stablilty and metastability, we feel their distinction in magnetism is unimportant in so far as the magnetization process is concerned. The ubiquitous phenomenon of magnetic hysteresis rests on the stability of a magnetic state regardless whether it is a ground or metastable state. In this regard, finding an energy-minimum state is sufficient and in fact even necessary in modelling of the behavior of magnetic particles.
[28] It is generally desirable to have the size of the finite elements to be a bit less than the exchange length of the material. In most of our calculations, they are. For larger disks (diameter $\geqslant$400 nm), the employment of such a fine mesh (mesh with less than the exchange length of the material) puts too much demand on memory requirements and computation time. The linear interpolation scheme used in our finite-element (as opposed to finite-different) calculations makes it more tolerable to have coarser meshes (meshes with nodal distances as large as twice the exchange length of the material). This was tested by calculating the

magnetic pattern in some of the smaller disks with both very coarse and fine meshes. These meshes yield the same magnetic state, except one shows more details than the other for the obvious reason.

[29] Note that Rothman *et al.* (Ref. 24) have also used the term onion state to describe a similar state in ring-shaped elements.

[30] Similar head-on domain structures have also been observed in rectangular elements. See Refs. 25 and 26.